5-15-2017

Laminar composite structures for high power actuators

M. A. Hobosyan

P. M. Martinez

A. A. Zakhidov

C. S. Haines

R. H. Baughman

See next page for additional authors

Recommended Citation

M. A. Hobosyan, et. al., (2017) Laminar composite structures for high power actuators.Applied Physics Letters110:20. DOI: http://doi.org/10.1063/1.4983028

This manuscript was accepted by Appl. Phys. Lett. Click here to see the version of record.

Laminar composite structures for high power actuators

M.A. Hobosyan[1], P. Martinez[2], A.A. Zakhidov[2,3], C.S. Haines[2], R.H. Baughman[2] and K.S. Martirosyan[1*]

[1]Department of Physics, University of Texas Rio Grande Valley, Brownsville, TX 78520, USA

[2]NanoTech Institute, University of Texas at Dallas, Richardson, TX 75083, USA

[3]Energy Efficiency Center, National University of Science and Technology, MISiS, Moscow, 119049, Russia

*karen.martirosyan@utrgv.edu

Twisted laminar composite structures for high power and large-stroke actuators based on coiled Multi Wall Carbon Nanotube (MWNT) composite yarns were crafted by integrating high-density Nanoenergetic Gas Generators (NGG) into carbon nanotube sheets. The linear actuation force, resulting from the pneumatic force caused by expanding gases confined within the pores of laminar structure and twisted carbon nanotube yarns, can be further amplified by increasing NGG loading and yarns twist density, as well as selecting NGG compositions with high energy density and large-volume gas generation. Moreover, the actuation force and power can be tuned by the surrounding environment, such as to increase the actuation by combustion in ambient air. A single 300-μm-diameter integrated MWNT/NGG coiled yarn produced 0.7 MPa stress and a contractile specific work power of up to 4.7 kW/kg while combustion front propagated along the yarn at velocity up to 10 m/s. Such powerful yarn actuators can also be operated in vacuum, enabling their potential use for deploying heavy loads in outer space, such as to unfold solar panels and solar sails.

This manuscript was accepted by Appl. Phys. Lett. Click here to see the version of record.

Introduction

Recent decades of advancement in nanotechnology enabled the development of nanoscale sensors and electromechanical devices, which are capable of active response through actuation. Various types of artificial muscles, based on actuation in nanofibers have been developed, particularly with carbon nanotube yarns and sheets [1]. Among the advanced actuator systems, the composites materials based on the carbon nanotubes are of exceptional importance. The enormous interest towards carbon nanotubes is driven by the outstanding physical and mechanical properties attractive for applications, particularly, the remarkable strength and high stiffness of up to 300 MPa for single-ply yarns [2], as well as extraordinary electrical, optical [3, 4] and thermal properties of carbon nanotubes [5]. These physical properties combined with high aspect ratio (length/diameter) and low density of carbon nanotubes inspired extensive research on developing advanced composite material systems. Specifically, Multi Walled Carbon Nanotube (MWNT) sheets extracted from carbon nanotube forest are opening a perspective for utilization in textile composite nanomaterials. It was shown that MWNT sheets can be scrolled into yarns incorporating functional materials, such as wax, where the yarns can act as actuators [6, 7] when electrically or optically changing the yarn temperature [8, 9]. Various solvents and water vapor can drive mechanical actuation in hierarchically arranged helical carbon nanotube fibers and yarns [10-12].

Combustion reactions can liberate high-pressure gasses at extremely high speeds, and this rapid gas expansion can potentially drive large-work, high-force actuation if confined within twisted MWNT yarns. Based on this strategy, we have created nanocomposites comprising twisted MWNT yarns that contain nanoenergetic guest-

This manuscript was accepted by Appl. Phys. Lett. Click here to see the version of record.

loaded materials, which act as Nanoenergetic Gas Generators (NGG) upon rapid combustion [13]. The NGG are nano-structured mixtures of fuel (metal nanoparticles, usually Al or Mg) and non-metal or metal oxides (Bi_2O_3, I_2O_5, Fe_2O_3 etc). In this study we employ the nanoenergetic system of Al-I_2O_5 due to superior generation of highly gaseous phases [14]. In applications where the toxicity of released iodine gas can be concerning, Al-$Bi(OH)_3$ NGG can be used [15], which releases large amount of water vapors and bismuth. In the medical, biological sciences and ceramic industry, bismuth and its compounds are considered as relatively safe. The in-vitro cytotoxicity of bismuth nanoparticles showed that the reason of low toxicity of bismuth nanoparticles is that the bismuth ions are the least toxic among all heavy metals [16]. The generated gases act as a pneumatic pump to rapidly inflate the MWNT yarns and produce tensile and torsional actuation owing to the twisted and coiled yarn structures. The proposed actuator yarns can be utilized in deployment of solar sails and panels, emergency forced opening of valves, elevation of heavy objects in hard to reach situations, where high power to mass ratio is desired.

Preparation of MWNT/NGG yarns

MWNT/NGG yarns were prepared by spray coating nanoenergetic composite of Al-I_2O_5 into 20 MWNT sheets and scrolling them into twisted and coiled yarns. The details of experimental methods and procedures are specified in the supplement. SEM of the stacked MWNT sheets before NGG coating reveals MWNT bundles preferentially aligned in the direction of the sheet with interconnected structure, Figure 1(a-d). When spraying the NGG suspension on the stacked sheets, the NGG particles stick on the

This manuscript was accepted by Appl. Phys. Lett. Click here to see the version of record.

surface of MWNT layers, Figure 1(b). The average size of the NGG agglomerates is about 1 μm.

To form MWNT/NGG yarns, the stacked sheets were twisted into Archimedean yarns, as described in ref [17], with 800-1000 turns/m per final yarn length. The coiled yarns were created by introducing further 2.5×10^4 turns/m, ref [8]. SEM images of the MWNT/NGG yarns reveal diameters between 350-400 μm for coiled yarns, while twisted yarns have a diameter of 250-300 μm as demonstrated in Figure 1(c, d). Matlab image analysis of the yarn cross-section reveals around 45 % porosity, with 55 % of the volume occupied by MWNTs and NGGs.

The yarns show excellent durability, with tensile stress values between 170-200 MPa for yarns containing 75-85 wt. % NGG, compared to about 227 MPa tensile stress value for pure MWNT yarn shown in the Figure 1(e). Thus, the typical actuator yarns retain about 75-90 % of initial MWNT strength. The addition of NGG in MWNT structure increases the yarn resistivity from ~ 10 mΩ*cm room temperature value to ~20 mΩ*cm value for yarns containing 75 wt. % of NGG presented in the Figure 1(f). When decreasing the temperature, the yarn resistivity gradually increases, which is in agreement with previously published experiments [18]. Reducing the temperature below 25 K results in sharper increase of resistivity with 21 mΩ*cm for MWNT yarn, and 50 mΩ*cm for MWNT yarn containing 75 wt. % Al-I_2O_5 NGG at 2.9 K temperature. Thus, if operated in space (~2.7 K), lower voltage may be required to ignite the NGG and generate yarn actuation.

This manuscript was accepted by Appl. Phys. Lett. Click here to see the version of record.

Actuation by the MWNT/NGG yarns

The ignition of the NGG composite by applying 15V across the yarns generates Joule heating that initiates the propagating temperature front within the twisted and coiled structures that releases high temperature escaping gases. The infrared temperature measurements show that the NGG reaction ignites at around 514 ºC (Figure S1a, and S.1.b) and the propagating combustion front temperature was above 700 ºC (Figure S1.c and S.1.d). These escaping gases pneumatically increase the volume of the yarns which generates the actuation force according to the reaction:

$$3I_2O_5(s) + 10Al(s) = 5Al_2O_3(s) + 6I(g) + \Delta H\ (-\ 6.22\ kJ/g) \qquad (1)$$

During combustion of the MWNT/NGG coiled and twisted yarns, iodine gas escapes the confined spaces between MWNT sheets increasing the yarn diameter, demonstrated by high speed camera and SEM images in Figure 2 (a, b). The diameters increased ~10 times in a time-span of 8-34 ms, causing a stroke force (~0.45 N) along the yarn length, Figure 2(a), blue arrows. After cooling, the yarn final diameter expended to a final 520 μm, a 90 % increase compared to 275 μm initial diameter value. In order to measure the actuation stroke of the MWNT/NGG coiled and twisted yarns, one end of the yarn was attached to an immobile base and the other end to the force sensor. Twisted yarns with MWNT/NGG mass ratio 1:2 produce a 0.45 N stroke force, while heavily coiled yarns ~ 0.2 N, Figure 2 (c). The twofold stroke force decrease for coiled yarns is attributed to the tight MWNT morphology, as discussed in supplement.

In another set of actuation performance, the yarn is allowed to change length, causing the physical actuation, as illustrated in Figure 3. One end of the yarn was attached to an immobile base and the other end to the tip of a cantilever with a known

This manuscript was accepted by Appl. Phys. Lett. Click here to see the version of record.

force constant (k=2.45 Nm^{-1}). The ignition of the yarns was initiated by applying 15V across the yarn, Figure 3a. This technique worked in various environments, including vacuum and nitrogen. The contraction of yarn length can reach 30-50 %. Figure 3b demonstrates the actuation, where the yarn with length of 4.9 cm had shortened by 1.6 cm (33 %). The released iodine vapors are escaping the yarn in 20-30 ms timeframe that can be seen in Figure 3b inset.

To confirm that the actuation is due to the escaping gas expanding the MWNT yarn, two identical yarns (75 wt. % NGG in MWNT yarn, twisted yarn with mass 4 mg; length 5.5 cm; diameter 300 μm), one with Al-I_2O_5 and other with Ni-Al were ignited by applying 15 V across the yarns. A 1 g mass was attached from the bottom to the yarn, while the top was constrained against motion. Combustion of the Ni-Al system did not produce any gaseous product [19] in comparison with Al-I_2O_5 system. The sample coded "NiAl-air" displays in Figure 3(c) no actuation during yarn combustion, while Al-I_2O_5/MWNT yarn shows a powerful actuation, when 1 g mass was lifted vertically upward at a speed 1 m/s, reaching a contraction of ~4 cm in 41 ms (Figure 3c, inset). We note that combustion temperatures of Ni-Al yarns are comparable to those of Al-I_2O_5. Thus, the comparison of gasless Ni-Al system with Al-I_2O_5 proves that the gas generation has critical role in yarn actuation. Specifically, for the system (1), the fast oxidation reaction releases vigorous amount of iodine, generating high pressure, which can be estimated using Kamlet-Jacobs theory [20-23]. The combustion front velocity and generated pressure are given by

$$V = A\varphi^{\frac{1}{2}}(1 + B\rho_0) \qquad (2)$$

$$P = K\rho_0^2\varphi \qquad (3)$$

This manuscript was accepted by Appl. Phys. Lett. Click here to see the version of record.

Where: $\varphi = NM^{\frac{1}{2}}Q^{\frac{1}{2}}, \quad , K = 1.558, A = 1.01, B = 1.30$ (4)

The combustion front velocity V is expressed in m/s, P is the pressure (GPa), N is the moles of the gas per gram of initial mixture (mol/g), M is the molar mass of the gas (g/mol), Q is the enthalpy of the reaction (cal/g) and ρ_0 is the loading density (g/cm^3) respectively. Using Equation 3, we calculated a combustion front velocity of ~2600 m/s for the system (1), which is in good agreement with the experimentally measured value of ~2000 m/s [14]. The pressure calculated for reaction (1), using equation (3), was 1.3 GPa (for details of calculation, see the supplement). Thus, upon ignition, the NGG system (1) produces powerful pneumatic actuation of the MWNT/NGG coiled and twisted yarns.

To estimate the power generated during the MWNT/NGG coiled and twisted yarns actuation, the setup of lifting a mass of 2 g shown in Figure 3c (inset) was used. Unlike the force stroke measurement, when the two ends of the yarn are fixed, the bottom end of the yarn rotates around the yarn axis during the actuation. The specific power was higher for coiled yarns due to torsional untwisting kinetic energy, which caused the mass to rotate during uplift. The highest specific power reaches 4700 W/kg during yarn actuation. These are 94 times higher than that of a typical mammalian muscle that is 50 W/Kg [24]. In comparison, the power output for helical fiber actuators was estimated as 49 W/kg [11], and the typical power output of carbon nanotube actuators is 10 W/kg, reaching maximum at 270 W/kg [24]. The comparison of the actuation performance in air, inert environment and vacuum is detailed in supplement. The actuation efficiency estimation show that less than 1 % of overall heating and chemical energy is transformed into the mechanical actuation due to extreme high rate of escaping gases penetrating through the yarns. Increasing the efficiency of the energy transformation to the

This manuscript was accepted by Appl. Phys. Lett. Click here to see the version of record.

mechanical actuation by enhancing numbers of outer layers of carbon nanotube sheets leads to demolition of actuator yarns. Thus, the easiest and fast penetration rate of the discharge gases is the significant element for operation of this type of actuators, for which the high power, twist and rotational movements at high speed operation in vacuum are the most attractive advantages, despite the low efficiency. Moreover, with this low efficiency, the power to mass ratio of yarns is still the highest among carbon based actuators.

MWNT/NGG yarns after the actuation

The infrared temperature measurements show that the propagating combustion temperature front in coiled and twisted MWNT/NGG yarns is above 700 ºC. Even though carbon nanotubes start oxidizing in air at temperatures ~ 450 °C [25], the fast combustion front propagation of the NGG in the MWNT yarn, ~10 m/s, and the small yarn diameter (~250-400 μm) allow the heat to dissipate rapidly with little damage of the MWNT yarns. I_D/I_G ratios were taken from the Raman shift of the MWNT/NGG yarns in order to characterize the quantity of defects present before and after actuation. An increase of this ratio signifies an increase of structural defects in the MWNT, where the D band ~ 1335 cm^{-1} represents the degree of disorder in graphitic materials and the G band the crystalline graphite peak ~ 1590 cm^{-1}, Figure 4a [25]. The I_D/I_G ratio increased from 1.04 to 1.14 for yarns before and after being actuated, suffering a ~10 % overall damage after being combusted. Further TEM analysis of the ignited MWNT/NGG yarns in Figure 4b revealed that the individual walls of the nanotubes were being broken due to the expansion of the yarn during the NGG ignition/gas generation.

This manuscript was accepted by Appl. Phys. Lett. Click here to see the version of record.

Conclusions

Robust laminar MWNT/NGG composite coiled yarns were fabricated by extreme twisting of carbon nanotube sheets covered with nano-energetic material such as Al-I_2O_5. In coiled yarns, both tensile and torsional actuations can be generated simultaneously by vigorous gas released during the combustion. The actuation force may potentially be improved by increasing the NGG loading density and the amount of twist inserted into the yarn. The contractile specific power was found to be greatest in air for coiled yarns and can be reached up to 4700 W/kg. According to Thermogravimetric, Raman and SEM analysis the structure of laminar twisted MWNT yarns is preserved after combustion and actuation. Ultimately, the proof-of-concept of a proposed laminar MWNT/NGG composites show a great potential to use as a one-time, high power and high stroke actuator materials that can work in both atmospheric and vacuum/inert conditions. The laminar composites can be used towards outer space applications for the deployment of solar sails and panels, to reduce the weight and complexity that accompany conventional actuators.

Supplementary Material

The supplementary material presents the details of MWNT/NGG yarn preparation, actuation force measurement setup, estimation of pressure and combustion front velocity, the performance comparison between coiled and twisted yarns, and infrared temperature measurements, SEM, TEM and DSC-TGA analysis of the yarns after combustion.

The supplementary video SV-1 shows twisting MWNT yarns from MWNT sheets that have been coated with NGG particles. The supplementary video SV-2 demonstrates

MWNT/NGG coiled yarn lifting a 2 g load by 2 cm, while simultaneously producing fast torsional actuation.

Acknowledgements

We would like to acknowledge the financial support of this research in part of the Army Research Office (grant No. 66389-CH-REP), the NSF PREM (award DMR-1523577: UTRGV-UMN Partnership for Fostering Innovation by Bridging Excellence in Research and Student Success), Welch Foundation grant 16-17 and CONACYT for academic opportunities and academic support. We also appreciate the partial support of the Ministry of Education and Science of the Russian Federation in the framework of Increase Competitiveness Program of NUST «MISiS» (K2-2015-014).

References

1. Baughman, Ray H., Anvar A. Zakhidov, and Walt A. de Heer. "Carbon nanotubes-the route toward applications." science 297, no. 5582 (2002): 787-792.
2. Zhang, Mei, Ken R. Atkinson, and Ray H. Baughman. "Multifunctional carbon nanotube yarns by downsizing an ancient technology." Science 306, no. 5700 (2004): 1358-1361.
3. Zakhidov, Anvar A., Ray H. Baughman, Zafar Iqbal, Changxing Cui, Ilyas Khayrullin, Socrates O. Dantas, Jordi Marti, and Victor G. Ralchenko. "Carbon structures with three-dimensional periodicity at optical wavelengths." Science 282, no. 5390 (1998): 897-901.
4. Ulbricht, Ross, Sergey B. Lee, Xiaomei Jiang, Kanzan Inoue, Mei Zhang, Shaoli Fang, Ray H. Baughman, and Anvar A. Zakhidov. "Transparent carbon nanotube sheets as 3-D charge collectors in organic solar cells." Solar Energy Materials and Solar Cells 91, no. 5 (2007): 416-419.
5. Aliev, Ali E., Csaba Guthy, Mei Zhang, Shaoli Fang, Anvar A. Zakhidov, John E. Fischer, and Ray H. Baughman. "Thermal transport in MWMWNT sheets and yarns." Carbon 45, no. 15 (2007): 2880-2888.
6. Baughman, Ray H., Changxing Cui, Anvar A. Zakhidov, Zafar Iqbal, Joseph N. Barisci, Geoff M. Spinks, Gordon G. Wallace, Alberto Mazzoldi, Danilo De Rossi, Andrew G. Rinzler, et al. "Carbon nanotube actuators." Science 284, no. 5418 (1999): 1340-1344.
7. Aliev, Ali E., Jiyoung Oh, Mikhail E. Kozlov, Alexander A. Kuznetsov, Shaoli Fang, Alexandre F. Fonseca, Raquel Ovalle, Márcio D. Lima, Mohammad H. Haque, Yuri

N. Gartstein, et al. "Giant-stroke, superelastic carbon nanotube aerogel muscles." science 323, no. 5921 (2009): 1575-1578.

8. Haines, Carter S., Márcio D. Lima, Na Li, Geoffrey M. Spinks, Javad Foroughi, John DW Madden, Shi Hyeong Kim, Shaoli Fang, Mônica Jung de Andrade, Fatma Göktepe, et al. "Artificial muscles from fishing line and sewing thread." science 343, no. 6173 (2014): 868-872.
9. Lima, Márcio D., Na Li, Monica Jung De Andrade, Shaoli Fang, Jiyoung Oh, Geoffrey M. Spinks, Mikhail E. Kozlov, Carter S. Haines, Dongseok Suh, Javad Foroughi, et al. "Electrically, chemically, and photonically powered torsional and tensile actuation of hybrid carbon nanotube yarn muscles." Science 338, no. 6109 (2012): 928-932.
10. Gu, Xiaogang, Qingxia Fan, Feng Yang, Le Cai, Nan Zhang, Wenbin Zhou, Weiya Zhou, and Sishen Xie. "Hydro-actuation of hybrid carbon nanotube yarn muscles." Nanoscale 8, no. 41 (2016): 17881-17886.
11. Chen, Peining, Yifan Xu, Sisi He, Xuemei Sun, Shaowu Pan, Jue Deng, Daoyong Chen, and Huisheng Peng. "Hierarchically arranged helical fibre actuators driven by solvents and vapours." Nat Nanotechnol 2015, 10, 1077-1083.
12. He, Sisi, Peining Chen, Longbin Qiu, Bingjie Wang, Xuemei Sun, Yifan Xu, and Huisheng Peng. "A Mechanically Actuating Carbon‐Nanotube Fiber in Response to Water and Moisture." Angew. Chem. Int. Ed. 2015, 54, 14880 –14884.
13. Martirosyan K. S., "Nanoenergetic gas generators, principle and applications," J. Materials Chemistry, vol. 21, pp. 9400-9405, 2011.

14. Martirosyan K. S., Wang L and Luss D., "Novel nanoenergetic system based on iodine pentoxide," Chem. Phys. Lett., vol. 483, pp. 107-110, 2009.

15. Hobosyan, Mkhitar A., Srbuhi A. Yolchinyan, and Karen S. Martirosyan. "A novel nano-energetic system based on bismuth hydroxide." RSC Advances 6, no. 71 (2016): 66564-66570.

16. Luo, Yang, Chaoming Wang, Yong Qiao, Mainul Hossain, Liyuan Ma, and Ming Su. "In vitro cytotoxicity of surface modified bismuth nanoparticles." Journal of Materials Science: Materials in Medicine 23, no. 10 (2012): 2563-2573.

17. Lima, Márcio D., Shaoli Fang, Xavier Lepró, Chihye Lewis, Raquel Ovalle-Robles, Javier Carretero-González, Elizabeth Castillo-Martínez, Mikhail E. Kozlov, Jiyoung Oh, Neema Rawat, et al. "Biscrolling nanotube sheets and functional guests into yarns." Science 331, no. 6013 (2011): 51-55. Zhang, Xiefei, Qingwen Li, Yi Tu, Yuan Li, James Y. Coulter, Lianxi Zheng, Yonghao Zhao, Qianxi Jia, Dean E. Peterson, and Yuntian Zhu. "Strong carbon-nanotube fibers spun from long carbon-nanotube arrays." small 3, no. 2 (2007): 244-248.

18. White, Jeremiah DE, Robert V. Reeves, Steven F. Son, and Alexander S. Mukasyan. "Thermal Explosion in Al−Ni System: Influence of Mechanical Activation." The Journal of Physical Chemistry A 113, no. 48 (2009): 13541-135.

19. Kamlet M. J. and Jacobs S. J., Chemistry of Detonations. I. Simple method for Calculating Detonation Properties of Carbon-hydrogen-nitrogen-oxygen Explosives, J. Chem. Phys., 1968, 48, 23.

20. Kamlet M. J. and Ablard J. E., Chemistry of Detonations. II. Buffered Equilibrium, J. Chem. Phys., 1968, 48, 36.

21. Kamlet M. J. and Dickinson C., Chemistry of Detonations. III. Evaluation of the Simplified Calculational Method for Chapman-Jouguet Detonation Pressures on the Basis of Available Experimental Information, J. Chem. Phys., 1968, 48, 43.

22. Geith, Janna, Thomas M. Klapötke, Jan Weigand, and Gerhard Holl. "Calculation of the Detonation Velocities and Detonation Pressures of Dinitrobiuret (DNB) and Diaminotetrazolium Nitrate (HDAT ‐ NO3)." Propellants, Explosives, Pyrotechnics 29, no. 1 (2004): 3-8.

23. Madden, John DW, Nathan A. Vandesteeg, Patrick A. Anquetil, Peter GA Madden, Arash Takshi, Rachel Z. Pytel, Serge R. Lafontaine, Paul A. Wieringa, and Ian W. Hunter. "Artificial muscle technology: physical principles and naval prospects." IEEE Journal of oceanic engineering 29, no. 3 (2004): 706-728.

24. Lehman, John H, Terrones Mauricio, Mansfield Elizabeth, Hurst Katherine E., Meunier Vincent. “Evaluating the characteristic of multiwall carbon nanotubes.” Carbon, no. 49 (2011): 2581-2602.

Figure 1. (a) SEM showing the morphology of 15 MWNT sheets stacked on top of each other, (b) SEM imaging of the same MWNT sheets after being coated with the nanoenergetic Al-I_2O_5. (c) SEM of the typical twisted yarn showing a diameter of 270 μm, (d) SEM of the typical coiled yarn with diameter of ~375 μm. (e) Tensile stress-strain curves for MWNT yarns without NGG, with 75 wt. % and 85 wt. % NGG loading. (f) Resistivity dependence on temperature for MWNT yarn without NGG and with 75 wt. % NGG

Figure 2. (a) The actuator yarn before combustion, the scheme of gas escape (red arrows) and actuation (blue arrows), and the yarn after actuation. (b) Snapshots showing the change in yarn diameter during gas generation, extracted from 240 fps IR filtered video recording. (c) Force sensor measurement over time for three type of yarns: simple twisted yarn with MWNT/NGG 1:2 mass ratio (red line), Coiled yarn with MWNT/NGG 1:2 mass ratio (green line) and twisted yarn containing 67 wt. % excess iodine pentoxide oxidizer (blue line).

Figure 3. (a) The snapshots showing yarn actuation evolution, extracted from 480 fps video recording; (b) The yarn length change during actuation: Initial yarn diameter 250 μm, tarn length 4.9 cm, final yarn diameter 450 μm, yarn length 3.6 cm. (insets) schematic diagram of actuation force measurement setup, and snapshot showing the gas escape during actuation; (c)**.** The environmental dependence on the stress and specific power during actuation of coiled yarn in air, nitrogen, vacuum, twisted yarn, and gasless combustion of a Ni-Al system in the twisted yarn, producing no actuation (the specific power is denoted with (*)), inset: Actuation of a 1 g mass load, left- ignition of the yarn, right- maximum 4 cm height achieved 41 ms after the ignition.

Figure 4. (a) Raman analysis of MWNT/NGG yarns before and after actuation, (b) individual MWNT with ruptured walls after actuation.

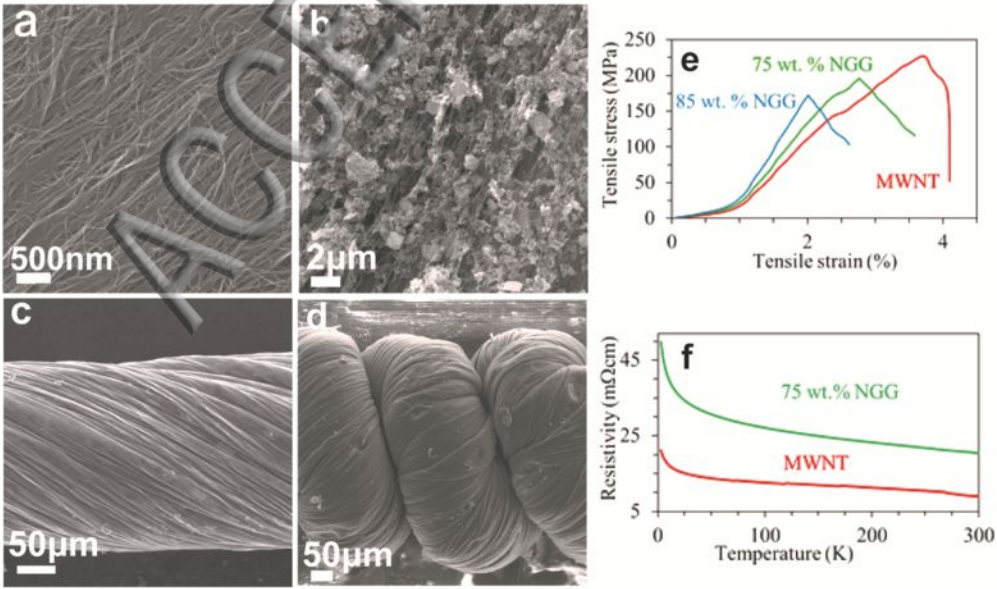
a
500nm
b
2μm
c
50μm
d
50μm
e
75 wt. % NGG
85 wt. % NGG
MWNT
Tensile stress (MPa)
Tensile strain (%)
f
75 wt.% NGG
MWNT
Resistivity (mΩcm)
Temperature (K)

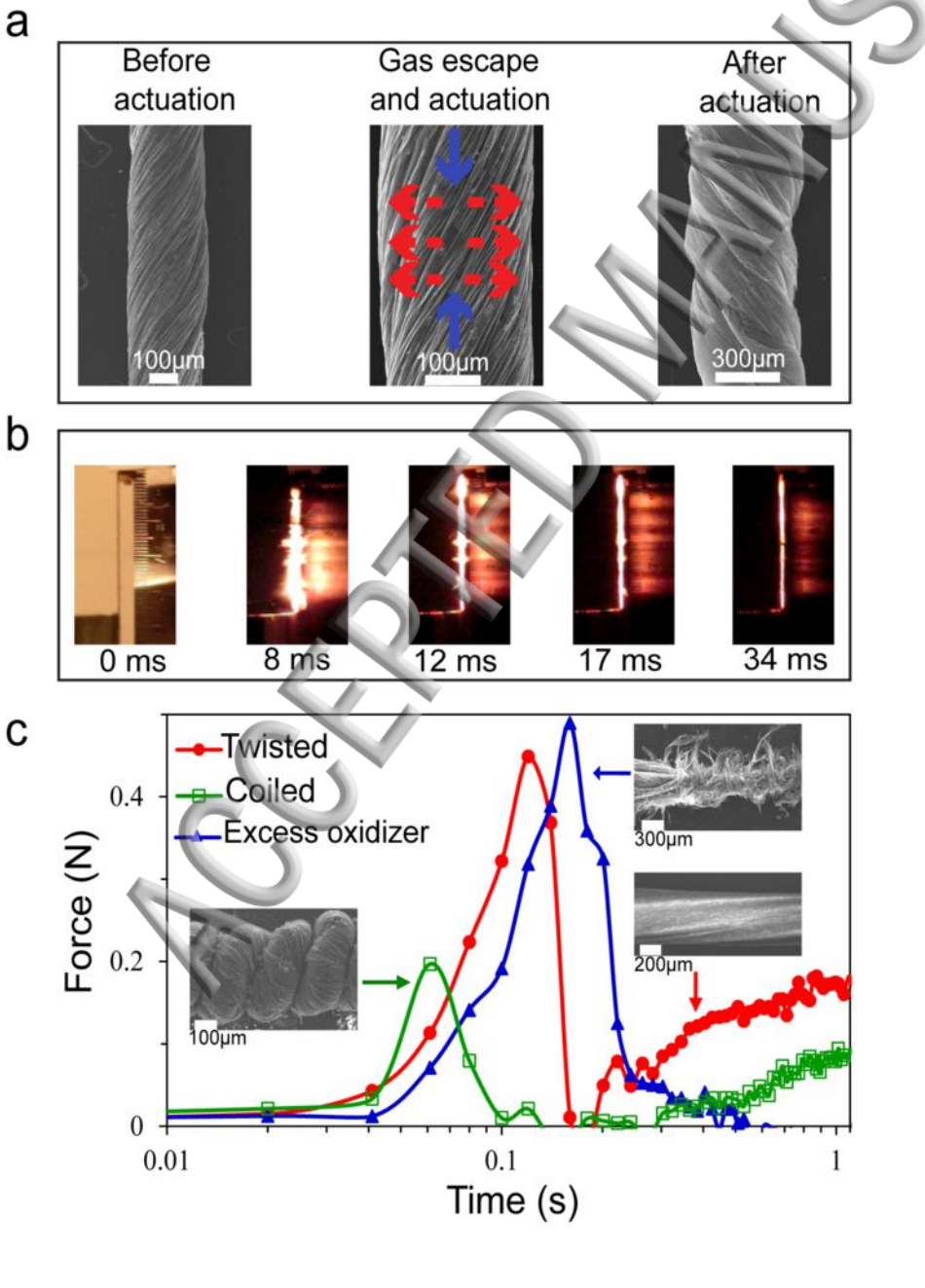

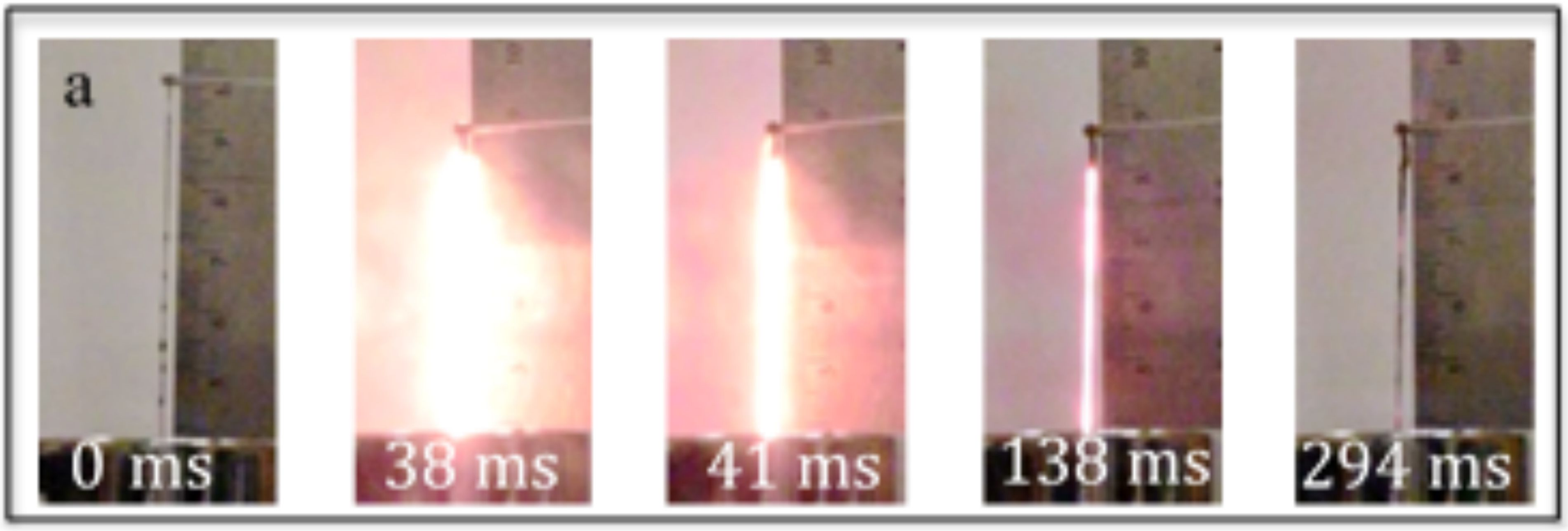

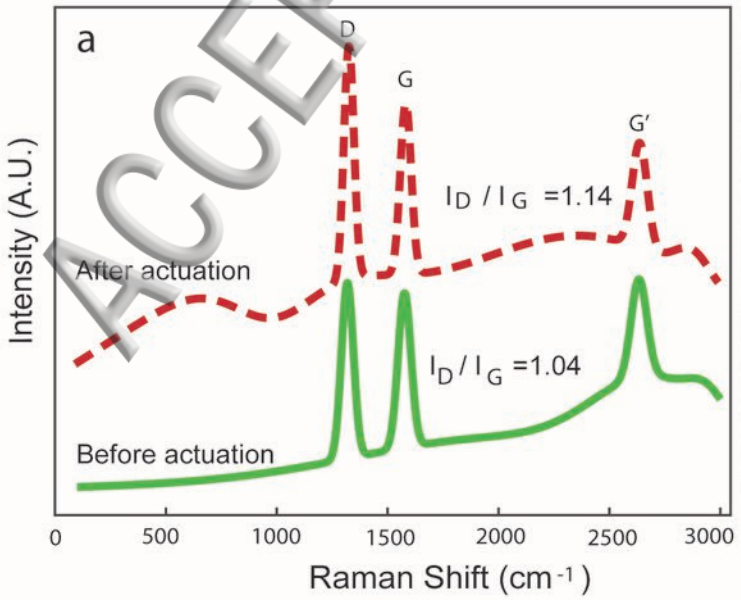
a
D
G
G′
I_D / I_G =1.14
After actuation
I_D / I_G =1.04
Before actuation
Intensity (A.U.)
0
500
1000
1500
2000
2500
3000
Raman Shift (cm^{-1})

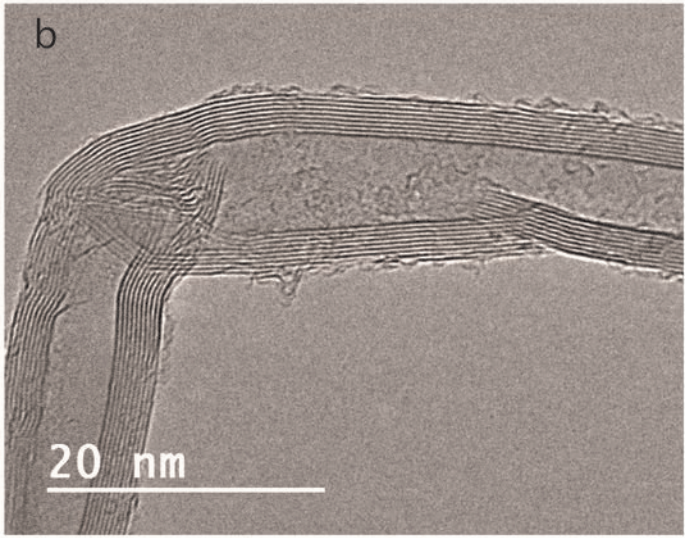
b
20 nm